Isotropic collision-induced light scattering by gaseous CF_4

A. Elliasmine,[1] J.-L. Godet,[1] Y. Le Duff,[1] and T. Bancewicz[2]
[1]*Faculté des Sciences, Laboratoire des Propriétés Optiques des Matériaux et Applications, Université d'Angers, 2 boulevard Lavoisier, 49045 Angers, France*
[2]*Nonlinear Optics Division, Institute of Physics, Adam Mickiewicz University, Umultowska 85, 61-614 Poznań, Poland*
(Received 4 November 1996)

The binary isotropic collision-induced scattering spectra of the gaseous tetrafluoromethane has been measured in absolute units in the 50–150 cm^{-1} frequency range. Corresponding theoretical intensities taking into account multipolar polarizabilities have been calculated in a semiclassical way. From a comparison with experiment, the independent components of dipole-quadrupole and dipole-octupole polarizability tensors have been estimated. They have been compared with those previously deduced from depolarized spectrum and with recent theoretical *ab initio* calculations. [S1050-2947(97)02706-6]

PACS number(s): 34.50.Gb, 33.20.Fb, 33.70.−w

I. INTRODUCTION

Collision-induced scattering (CIS) in fluids arises from polarizability variations caused by interactions between molecules [1]. For low-density fluids, interactions are binary and CIS comes from collisional polarizabilities of the molecular pairs. In the case of gases consisting of optically isotropic molecules, pure collision-induced depolarized spectra are observed in the vicinity of the Rayleigh line where no monomolecular scattering is allowed [2,3]. Information on the molecular interactions may be obtained from these spectra. For the lower-frequency part of these collision-induced depolarized spectra, the dipole-induced-dipole (DID) interaction accounts for most of the observed scattering intensities, whereas, at high-frequency shifts, multipole polarizabilities have to be taken into account and play a leading role [3]. For isotropic *molecules* the excess polarizability induced by interactions in a pair is a tensor that has two invariants: its anisotropy $\beta(r)$ and its trace $\alpha_t(r)$ related to the depolarized and the isotropic CIS, respectively. From intensity measurements of depolarized CIS spectra, anisotropy models have been proposed for several pairs of identical isotropic molecules (CH_4, SF_6, and CF_4) [3–5]. However, up to now, no isotropic CIS spectra have been reported for globular molecules and the trace of the collisional polarizability tensor of dimers involving such molecules is not available.

It is the purpose of our present work to study the isotropic CIS spectra for pairs of CF_4 and to deduce information on the molecular interactions that contribute to the trace of the collision-induced polarizability tensor for a pair of CF_4 molecules. In particular, the influence of successive multipolar contributions is considered. After a presentation of the experimental procedure and theoretical fundamentals based on semiclassical principles (which do not take into account quantum effects such as overlap and exchange), a comparison between experimental and theoretical results is performed. Values for the independent components of the dipole-quadrupole and dipole-octupole polarizability tensors are obtained. Finally, we discuss the coherence of the latter results with those deduced by us earlier from the depolarized spectrum [5] and those recently computed *ab initio* by Maroulis [6,7].

II. EXPERIMENT

The scattered intensities have been measured at 294.5 K using a typical scattering experimental setup described previously [8]. We used the green line (514.5 nm) of an argon laser to illuminate the gas sample contained in a four-window high-pressure cell. The CF_4 gas was provided by L'Air Liquide with a purity of 99.995%. Before using this gas for the experiment, we subjected it to thermal purification in order to eliminate traces of air, which could affect our measurements. Densities were deduced from *PVT* data given in Ref. [9]. The scattered radiation was collected at 90° within a solid angle of 6.2° and then detected with a low dark-noise bialkali photomultiplier connected to a photon counter. In order to obtain the isotropic intensities we measured two types of scattering intensities $I_H(\nu)$ and $I_V(\nu)$, recorded with an incident laser beam polarization parallel and perpendicular, respectively, to the scattering plane (defined by the laser beam and the axis of the scattered beam). The change of laser polarization was obtained using a half plate associated with a Glan polarizer. No analyzer was used for the scattering beam. We calculated the isotropic intensity $I_{\mathrm{iso}}(\nu)$ using [10,11]

$$I_{\mathrm{iso}}(\nu)=\left[\frac{d-b\,\eta_n(\nu)}{c\,\eta_n(\nu)-a}\right]I_d(\nu), \tag{1}$$

where $\eta_n(\nu)=I_H(\nu)/I_V(\nu)$ is the observed depolarization ratio and $I_d(\nu)$ the depolarized scattering intensity [5]. a, b, c, and d are coefficients dependent on the collection scattering angle Θ_c [11]. Since Θ_c was relatively small in our experiments ($\Theta_c=6.2°$), we had $a \ll c\,\eta_n(\nu)$ and

$$I_{\mathrm{iso}}(\nu)=\left[\frac{1.004}{\eta_n(\nu)}-1.1695\right]I_d(\nu). \tag{2}$$

Then, using the CF_4 intensities $I_d(\nu)$ measured previously in absolute units [5] and depolarization ratio values, the isotropic intensities have been directly obtained in absolute units from Eq. (2). For each experimental intensity a spectral correction was applied to take into account the change in sensitivity of our apparatus (double monochromator plus detector) with wavelength.

III. ISOTROPIC COLLISION-INDUCED SCATTERING MECHANISMS

For a laser beam polarized in the scattering plane and detected with no analyzer the theoretical isotropic light scattering double differential cross section is given by [12]

$$\left(\frac{\partial^2\sigma}{\partial\Omega\,\partial\omega}\right)_{\rm iso}=\frac{1}{3}\,k_i k_s^3\,\frac{1}{2\pi}\int \exp(-i\omega t)F_{00}(t)dt, \quad (3)$$

where

$$F_{00}(t)=\langle \mathsf{A}_0(0)\odot\mathsf{A}_0(t)\rangle \quad (4)$$

denotes the autocorrelation function of the irreducible spherical isotropic component of the pair polarizability tensor. In Eq. (4) $\odot$ stands for the scalar tensor product and $\langle\ \rangle$ is a canonical average.

The pair polarizability tensor A_0 splits into two parts

$$\mathsf{A}_0={}_{(M)}\mathsf{A}+\Delta\mathsf{A}_0, \quad (5)$$

the isotropic polarizability of two monomers ${}_{(M)}\mathsf{A}_0$ and the excess pair polarizability originating in intermolecular interactions $\Delta\mathbf{A}_0$. The excess spherical irreducible pair polarizability tensor ΔA_{KM} can be easily calculated by standard methods of statistical mechanics and angular-momentum theory (see the Appendix). In the space fixed laboratory frame it can be written in the form (the most adequate for our calculations)

$$\Delta A_{KM}=\sqrt{4\pi}\sum_{\substack{j_1,j_2,N\\ l_1,l_2}} A^{(K)}_{j_1 j_2 x N}R_{12}^{-(N+1)} \times\{\mathsf{Y}_N(\mathsf{R}_{12})\otimes[\alpha^{(1,l_1)}_{j_1}(1)\otimes\alpha^{(1,l_2)}_{j_2}(2)]_x\}_{KM}, \quad (6)$$

where $\alpha^{(1,l_i)}_{j_i}(i)$ is the irreducible j_ith rank spherical tensor of the dipole–l_ith rank multipole polarizability of a molecule i, $\otimes$ denotes the irreducible spherical tensor product, and Y_N stands for the spherical harmonic function. The nonzero coefficients $A^{(0)}_{j_1 j_2 N N}$ of Eq. (6), up to order R_{12}^{-7}, for the isotropic component ΔA_{00} of the excess interaction-induced polarizability are assembled in the Appendix. For tetrahedral molecules, in contrast to the anisotropic scattering [5], effects arising from nonlinear polarization in the strong electromagnetic field, up to order R_{12}^{-7}, do not contribute to the isotropic pair polarizability.

When considering radiation scattered by low-density gaseous systems with almost spherical CF_4 potential, it is generally justified to assume that the molecules of the scattering volume are radially correlated but orientationally uncorrelated. Then, using Eqs. (4) and (6) and isotropically averaging over the initial orientations of molecules 1 $[\Omega_1(0)]$ and 2 $[\Omega_2(0)]$ as well as over the initial orientation $\Omega_{12}(0)$ of the intermolecular vector for $F_{00}(t)$ we obtain

$$F_{00}(t)=\sum_{\substack{j_1,j_2,N\\ l_1,l_2}}\frac{3}{(2j_1+1)(2j_2+1)} \times|A^{(0)}_{j_1 j_2 N N}|^2(\tilde{\alpha}^{(1,l_1)}_{j_1}\odot\tilde{\alpha}^{(1,l_1)}_{j_1}) \times(\tilde{\alpha}^{(1,l_2)}_{j_2}\odot\tilde{\alpha}^{(1,l_2)}_{j_2})S_N(t)R_{j_1}(t)R_{j_2}(t), \quad (7)$$

where [5]

$$S_N(t)=\langle D^N_{00}(\delta\Omega_{12}(t))R_{12}(0)^{-(N+1)}R_{12}(t)^{-(N+1)}\rangle, \quad (8)$$

$$R_j(t)=\langle D^j_{nn}(\delta\Omega(t))\rangle, \quad (9)$$

with $D^j_{mn}(\Omega)$ standing for the Wigner matrix [13] and $\delta\Omega(t)$ and $\delta\Omega_{12}(t)$ denoting the reorientational angles at time t of the molecule and intermolecular vector, respectively. The tilde denotes the multipolar polarizability tensor in the frame of the principal axes of a molecule. From Eq. (7) it results that knowledge of the pair polarizability expansion coefficients $A^{(0)}_{j_1 j_2 N N}$ and molecular frame multipolar polarizability irreducible spherical components enables us to calculate the spectral line shape of the isotropic part of the scattered radiation. The isotropic light scattering correlation functions resulting from Eq. (7) for successive multipolar induction operators are assembled in Table I.

TABLE I. Isotropic light scattering correlation functions $F_{00}(t)$ for successive multipolar induction operators.

Mechanisms	$F_{00}(t)$
$\alpha\mathsf{T}\alpha\mathsf{T}\alpha$	$48\alpha^6 S_0(t)$
$\alpha\mathsf{TA}$	$\frac{160}{7}\alpha^2A^2S_3(t)R_0(t)R_3(t)$
$\alpha\mathsf{TE}$	$\frac{224}{9}\alpha^2E^2S_4(t)R_0(t)R_4(t)$
ATA	$\frac{1408}{189}A^4S_4(t)R_3(t)R_3(t)$
ATE	$\frac{416}{21}A^2E^2S_5(t)R_3(t)R_4(t)$
ETE	$\frac{55}{3}E^4S_6(t)R_4(t)R_4(t)$

When using spherical top wave functions for the evaluation of transition matrix elements, the Fourier transform of $R_{j_1}(t)R_{j_2}(t)$ has the form [14]

$$\mathcal{F}_t[R_{j_1}(t)R_{j_2}(t)]=\frac{(2J_1+1)(2J_2+1)(2J_1'+1)(2J_2'+1)}{Z_1Z_2} \times\exp\left[-\frac{(E_{J_1}+E_{J_2})}{k_BT}\right]\delta(\omega-\omega_{J_1J_2J_1'J_2'}), \quad (10)$$

where

$$\omega_{J_1J_2J_1'J_2'}=-[J_1'(J_1'+1)+J_2'(J_2'+1) -J_1(J_1+1)-J_2(J_2+1)]B. \quad (11)$$

B is the rotational constant and Z_i denotes the rotational partition function. The selection rules have the form

$$\Delta J_1 = 0, \pm 1, \pm 2, \ldots, \pm j_1, \quad J_1 + J_1' \geqslant j_1 \tag{12}$$

$$\Delta J_2 = 0, \pm 1, \pm 2, \ldots, \pm j_2, \quad J_2 + J_2' \geqslant j_2. \tag{13}$$

We calculate the rotational stick spectrum of each multipolar mechanism using Eqs. (10)–(13). The successive light scattering contributions are then obtained by convoluting each stick spectrum with the corresponding translational one. These contributions are not very sensitive to the profile of the translational spectral component, which mainly serves to fill in the intensity between the sticks [15] and to provide an absolute spectrum. Therefore, following the procedure that we have previously employed [5], we simply make use of the Birnbaum-Cohen (BC) formula [16] in order to model the translational parts involved. This implies the computation of translational spectral moments for a given intermolecular potential. Several CF_4 potentials are available. Lennard-Jones [17–19] and Kihara [18] potentials have been tested in this work. In addition, for the BC formula different choices of moments may be done: either the classical zero-, second-, and fourth-order translational spectral moments [20,21] or semiclassical moments of zeroth, first, and second order [22]. However, as expected for a relatively large molecule such as CF_4, the quantum corrections to the zero- and second-order moments are less than 1% whatever the multipolar mechanisms and the used potential interactions are; we have found that the CF_4 Birnbaum-Cohen spectral profiles do not differ significantly for both methods (classical and semiclassical) and these will be treated in what follows without distinction.

IV. RESULTS AND DISCUSSION

We measured the $I_H(\nu)$ and $I_V(\nu)$ intensities that are scattered by the gaseous CF_4 up to 340 cm^{-1}, in the 2–105 amagat density range and at 294.5 K. A typical $I_H(\nu)$ spectrum obtained at 20.3 amagat is shown in Fig. 1. It exhibits two weak bands at about 200 and 280 cm^{-1}, which may be attributed to combinations between fundamental vibrational frequencies [23]. For several frequency shifts we have plotted the ratios $I_H(\nu)/\rho$ and $I_V(\nu)/\rho$ versus the density ρ as shown in Fig. 2 for $I_V(\nu)/\rho$ at $\nu = 20$, 30, 40, 110, and 130 cm^{-1}. Except for the low frequencies, for which a negative contribution due to the three-body processes appears at high pressures (for frequencies below 20 cm^{-1} and pressures above 40 amagat), it is clear that I_V ($\nu < 150$ cm^{-1}) is proportional to ρ^2 [this behavior had also been observed previously for the I_H ($\nu < 150$ cm^{-1}) values [5]]. From these curves, we have deduced the pair contributions $I_V^p(\nu)$ and $I_H^p(\nu)$ to the scattered intensities $I_V(\nu)$ and $I_H(\nu)$ and deduced the pair depolarization ratio $\eta^p(\nu) = I_H^p(\nu)/I_V^p(\nu)$, given in Fig. 3 up to 150 cm^{-1}. We do not provide $\eta^p(\nu)$ beyond 150 cm^{-1} since in the frequency range of the two Raman bands, namely, at ≈ 200 and ≈ 280 cm^{-1}, the spectral intensities vary linearly with the gas density and therefore are not of collision-induced nature (the depolarization ratio of these two bands are $\approx \frac{6}{7}$). On the contrary, below 150 cm^{-1}, the intensities are completely induced by molecular interactions and the depolarization ratio acquires a decreasing tendency with frequency, from $\frac{6}{7}$ (which is the expected depolarization ratio of a completely depolarized spectrum) to less than ≈ 0.4. This is in conformity with the following ascertainments: (i) the weakness of the DID isotropic light scattering mechanism, for which the isotropic part of the first-order DID, $\alpha \mathsf{T} \alpha$ mechanism is zero and therefore the corresponding η is $\frac{6}{7}$ (it is noteworthy that the isotropic part of the second-order DID, $\alpha \mathsf{T} \alpha \mathsf{T} \alpha$ mechanism is relatively weak and alone yields a depolarization ratio $\eta = \frac{2}{9} \approx 0.22$), and (ii) the leading role, with increasing ν, of the dipole-multipole mechanisms such as the dipole-quadrupole ($\alpha \mathsf{TA}$) and the dipole-octupole ($\alpha \mathsf{TE}$) mechanisms, for which the depolarization ratios are $\frac{9}{23} \approx 0.39$ and $\frac{22}{63} \approx 0.35$, respectively [24].

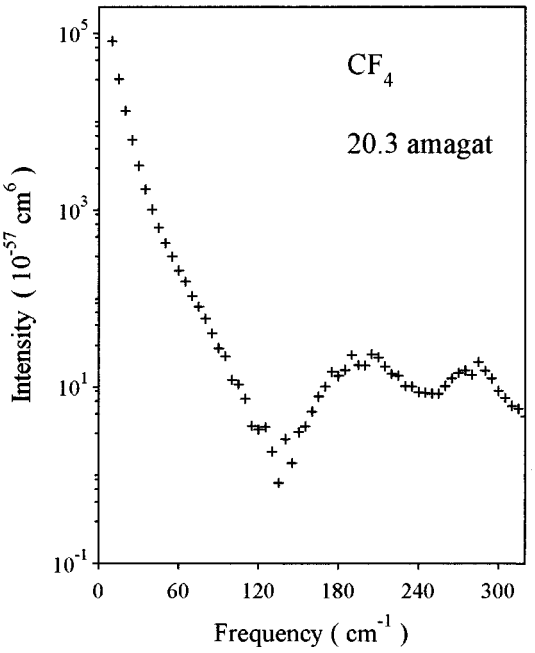

FIG. 1. Experimental depolarized intensities $I_H(\nu)$ in absolute units (cm^6) for the Stokes scattering of CF_4 gas versus frequency shifts in cm^{-1} at 20.3 amagat and 294.5 K.

Having provided the function $\eta^p(\nu)$ and the pair depolarized absolute intensities $I_d(\nu)$, pair isotropic absolute intensities can be deduced from Eq. (2). We report them in Fig. 4 together with error bars. The uncertainties are generally substantial, especially for the lowest and highest frequencies studied. This is mostly due to the fact that the isotropic spectrum is deduced by the substraction of two quantities close to each other as $\eta^p(\nu)$ goes to the value $\frac{6}{7}$ at low frequencies and relatively weak as $\eta^p(\nu)$ goes to ≈ 0.4 at high frequencies. Thus the intensities indicated by squares in Fig. 4 (for frequencies below 40 cm^{-1}) represent estimations rather than real measurements. Nevertheless, the pair isotropic intensities have been measured within satisfactory accuracy in the 50–150 cm^{-1} frequency range and may be compared with theoretical models. In the same Fig. 4, we report the theoretical $\alpha \mathsf{T} \alpha \mathsf{T} \alpha$ (second-order DID), $\alpha \mathsf{TA}$ [dipole-induced-quadrupole (DIQ)], $\alpha \mathsf{TE}$ [dipole-induced-octupole (DIO)], and $\mathsf{ATA} + \mathsf{ATE} + \mathsf{ETE}$ contributions to the isotropic spectrum for the polarizability value $\alpha = 2.93$ $Å^3$ (extrapolated at 514.5 nm from the data provided in Ref. [25]), a 12-6 Lennard-Jones potential [17], and the following choice of

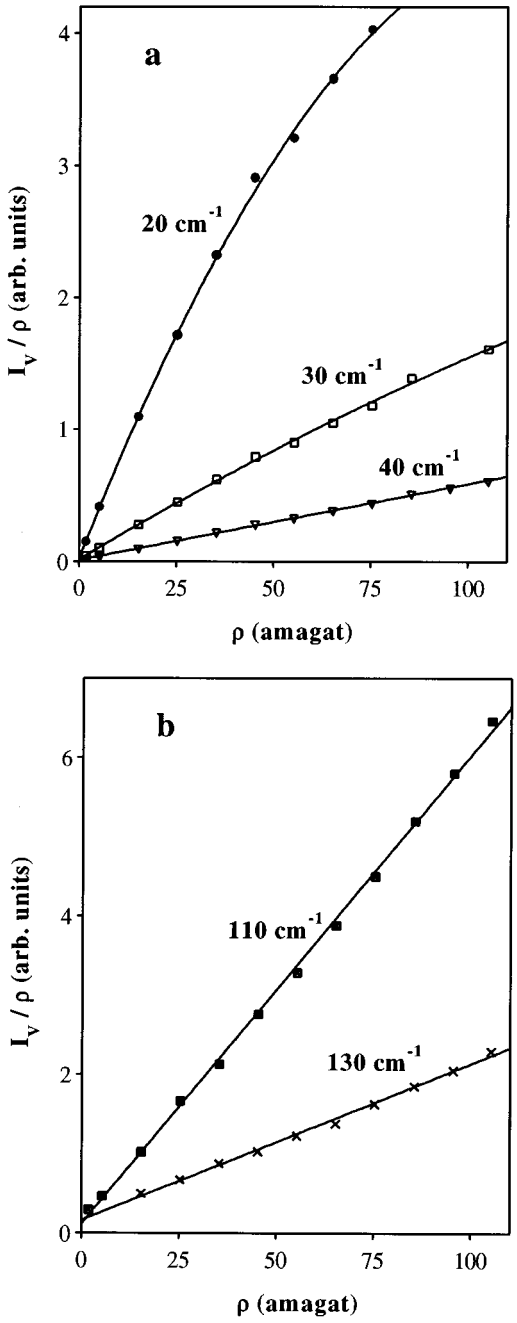

FIG. 2. Experimental polarized intensities $I_V(\nu)$ (arbitrary units) divided by density ρ versus ρ in amagat units for several frequency shifts: (a) 20, 30, and 40 cm^{-1} and (b) 110 and 130 cm^{-1}.

independent components A and E of the corresponding multipolar polarizability tensors: $|A|=0.7$ Å^4 and $|E|=2.5$ Å^5. These values give the best fit between the experimental and theoretical spectra. We found similar results for the other quoted Lennard-Jones and Kihara potentials [18,19]. Considering the error bars and the mutual competition of the αTA and αTE contributions, it is nonetheless obvious that the latter choice of $|A|$ and $|E|$ is not unique. On the other hand, we have calculated the *maximum* values of $|A|$ and $|E|$ resulting from the CIS isotropic spectrum. We define A_{max} as the maximum value of $|A|$ for which the αTA contribution *alone* (without any contribution from DID or αTE mechanisms) remains lower than or equal to the upper

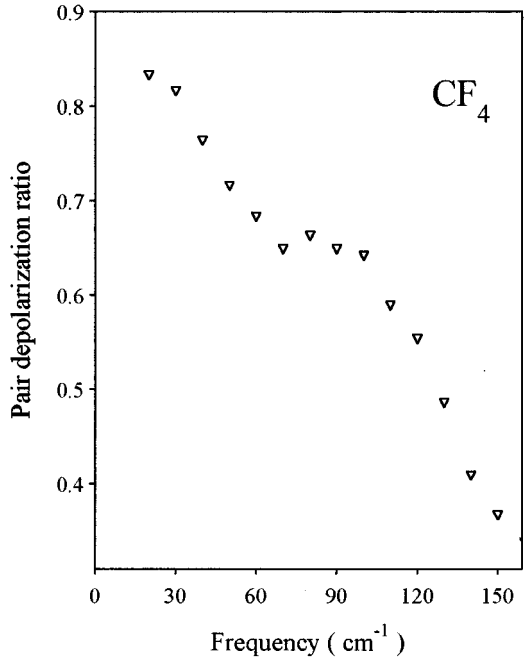

FIG. 3. Experimental pair depolarization ratio $\eta^p = I_H^p / I_V^p$ versus frequency shifts in cm^{-1} for the two-body CIS of gaseous CF_4 at 294.5 K.

error-bar limits of the experimental spectrum whatever the frequency is. A similar procedure is followed in order to determine E_{max}. Moreover, assuming that the multipolar mechanisms are predominant in the 50–150 cm^{-1} frequency range, an approximate estimation of the corresponding

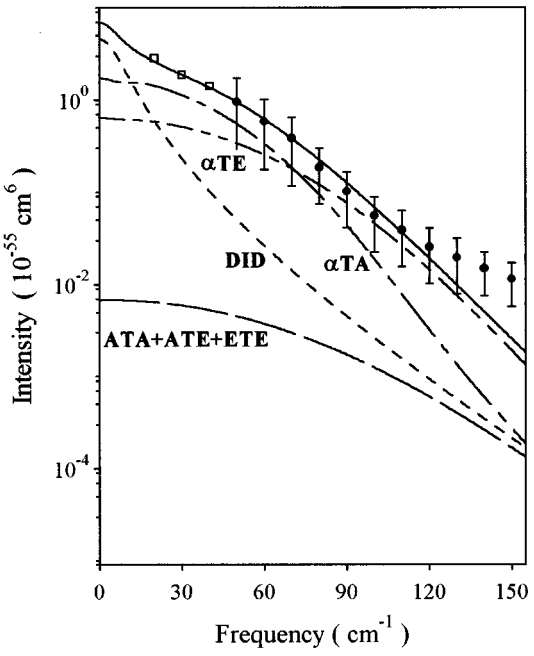

FIG. 4. Two-body *isotropic* scattering spectrum for CF_4 gas at 294.5 K. The full circles (●) indicate our experimental data with error bars; squares (□) are estimated data. Theoretical curves are provided for several contributions using $\alpha=2.93$ Å^3, $A=0.7$ Å^4, and $E=2.5$ Å^5: DID (---), αTA (— - —), αTE (— - - —), ATA + ATE + ETE (— —), as well as total theoretical intensities (——).

TABLE II. Theoretical and experimental fitted values of the independent components $|A|$ and $|E|$ of the dipole-quadrupole and dipole-octupole polarizability tensors, respectively, for the CF_4 molecule. The intermolecular potentials used for the calculations are either 12-6 Lennard-Jones (LJ) or Kihara potentials.

Method	Potential	$\|A\|$ (Å^4)	$\|E\|$ (Å^5)	Reference
Theory				
bond model		2.2	3.5	[3]
ab initio		0.97	1.15	[6, 7]
Experiment				
depolarized CIS	LJ [17]	2.2	2.2	[26]
depolarized CIS	LJ [17]	0.5–1.7	2.5–4.3	[5]
depolarized CIS	Kihara [18]	0.4–1.4	1.4–3.3	this work
isotropic CIS	LJ [17–19]	0.5–1.2	1.0–3.5	this work
isotropic CIS	Kihara [18]	0.3–1.0	1.0–2.5	this work

minima is possible. For example, we set $|E|=E_{\max}$ and take $A_{\min}$ as the largest value of $|A|$ for which the *total* theoretical spectrum remains lower than or equal to the upper error-bar limits of the experimental spectrum for any frequency. We repeat this procedure for $E_{\min}$. The intervals $[A_{\min}, A_{\max}]$ and $[E_{\min}, E_{\max}]$ are provided in Table II first for the cited Lennard-Jones potentials [17–19] and then for the Kihara potential [18], which gives slightly different results. They can be compared with those deduced in a similar manner [5] from the study of the experimental depolarized spectrum as well as with the fitted values of a previous measurement of the CF_4 depolarized spectrum [26]. Also in Table II we have

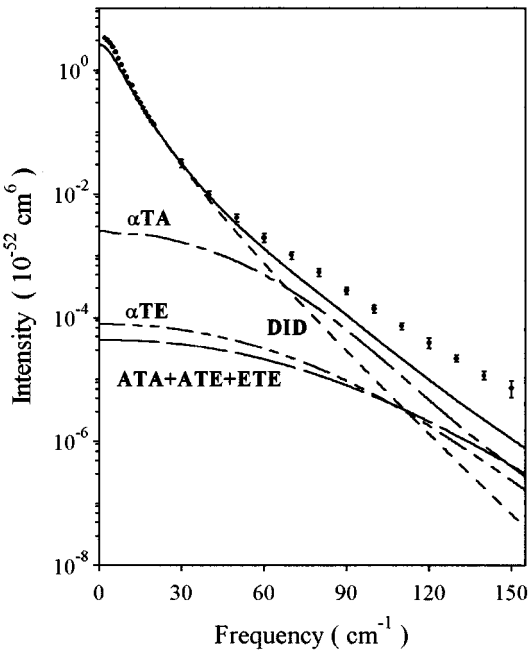

FIG. 5. Two-body *depolarized* scattering spectrum for CF_4 gas at 294.5 K. The full circles (●) indicate experimental data [5] with error bars. Theoretical curves are provided for several contributions using $\alpha=2.93$ Å^3, $A=1$ Å^4, and $E=1.5$ Å^5: DID (---), αTA (— - —), αTE (— - - —), ATA+ATE+ETE (— —), as well as total theoretical intensities (——).

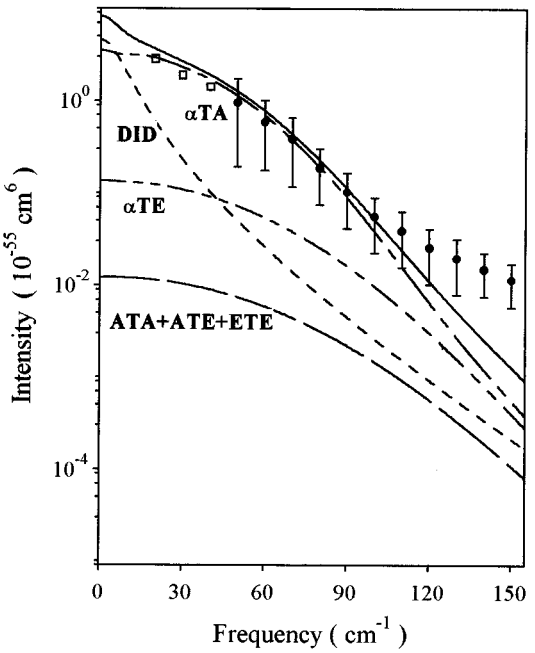

FIG. 6. Two-body *isotropic* scattering spectrum for CF_4 gas at 294.5 K. The full circles (●) indicate our experimental data with error bars; squares (□) are estimated data. Theoretical curves are provided for several contributions using $\alpha=2.93$ Å^3, $A=1$ Å^4, and $E=1.5$ Å^5: DID (---), αTA (— - —), αTE (— - - —), ATA+ATE+ETE (— —), as well as total theoretical intensities (——).

reported the theoretical values deduced from the rough bond polarizability model [3,27] and those recently calculated *ab initio* by Maroulis (i.e., his ''best or recommended'' SCF values taking into account electron correlation corrections) [6,7]. The two intervals of $|A|$ values deduced from our depolarized and our isotropic data partly overlap with each other for both types of potentials (Lennard-Jones or Kihara). This is also the case for two corresponding intervals of the $|E|$ values. We may note that the ''best fit'' of the CIS isotropic spectrum shown in Fig. 4 is obtained for values that are within the intervals deduced from our depolarized spectrum [5]. Also, the $A=0.97$ Å^4, computed by Maroulis, belongs to the two intervals $[A_{\min}, A_{\max}]$ obtained from depolarized and isotropic spectra, respectively. When this Maroulis value is assumed for A, our best choice for both the calculated depolarized and isotropic spectra correspond to $|E|=1.5\pm0.5$ Å^5, as shown in Figs. 5 and 6 for the Lennard-Jones potential given in [17]. The result is nearly the same as the Kihara potential for which we obtain $|E|=1.0\pm0.5$ Å^5. These values are coherent with the one ($E=-1.15$ Å^5) computed *ab initio* by Maroulis, although he provides static values for the polarizabilities [6,7], whereas in our study dynamic ones would be preferable. Finally, Maroulis's A and E are coherent with our isotropic spectrum (Fig. 6) as well as with our depolarized one (Fig. 5). However, with the values $|A|=1$ Å^4 and $|E|=1.5$ Å^5, we observe in Figs. 5 and 6 that the highest-frequency theoretical intensities are smaller than the experimental ones, for the depolarized spectrum for frequencies beyond 50 cm^{-1} and for the isotropic one beyond 120 cm^{-1}. In our opinion this may be, at least partly, due to two sources of incertitude for

our theoretical spectra: (i) short-range effects (such as overlap and exchange processes, molecular distortion, and/or spatial charge distribution of the non-point-like CF_4 molecule), which should be superimposed to the classical DID and dipole-multipole mechanisms and contribute especially to the high-frequency spectrum of each contribution [28], and (ii) the overall simplicity of the Lennard-Jones or Kihara potentials used in our calculations.

For CF_4, the numerical details of short-range contributions are not as yet available. In particular, the influence of the short-range effects on the pure translational contributions to the CIS spectra is not known. In our model, we take into account only the classical DID mechanism. However, as shown in Figs. 4–6, the DID contribution to the trace is weak even in the low-frequency range of the *isotropic* spectrum. Figure 5 shows that for the depolarized scattering the DID contribution plays the leading role below 50 cm^{-1} with good agreement between theory and experiment (except in the $0-15$ cm^{-1} frequency range where the contribution of bound and metastable dimers is not considered [5]). Nevertheless, there is no indication that this DID model for the depolarized spectrum is still a good description of the pure translational contribution beyond 50 cm^{-1}, where the dipole-multipole mechanisms become predominant. A significant increase of the computed pure translational intensities due to short-range effects in the $50-120$ cm^{-1} frequency range would affect the ''depolarized spectrum fit'' of the $|A|$ and $|E|$ values (see Fig. 5). It is the reason why the measurements of the dipole-quadrupole and dipole-octupole polarizabilities of a T_d-symmetry molecule such as CH_4 or CF_4 found through a comparison of a single depolarized CIS spectrum with experiment are uncertain. In contrast, Figs. 4 and 6 show that the pure translational part of the isotropic spectrum is very small and cannot perturb the ''isotropic spectrum fit'' of the dipole-multipole tensor components. Therefore, despite its larger uncertainties, the isotropic spectrum is the most adapted to obtain the $|A|$ value and to estimate the $|E|$ one.

V. CONCLUSION

Previously, absolute unit CIS isotropic spectra for atoms, rare gas homonuclear diatoms [29,11], and hydrogen and deuterium [30,28,31] have been reported. Here the trace binary CIS spectrum of optically isotropic molecules—in this case, of gaseous CF_4—has been measured in absolute units, in the $50-150$ cm^{-1} frequency range. We have shown that this very weak spectrum may be calculated theoretically mainly as a result of two dipole-multipole mechanisms, namely, the dipole-quadrupole $\alpha\mathsf{TA}$ and the dipole-octupole $\alpha\mathsf{TE}$ mechanisms. A comparison with previous measurements of the depolarized CIS spectrum of CF_4 [5] has been performed. We obtain the following ranges for A and E values: $|A|=0.5-1.2$ $Å^4$ and $|E|=1.0-3.5$ $Å^5$. The *ab initio* computed A value of Maroulis [6,7] ($A=0.97$ $Å^4$) is coherent with all our data. When this value is used for A, the maximum $|E|$ value that can be assigned for both depolarized and isotropic spectra is $|E|\approx 1.5\pm 0.5$ $Å^5$, whereas Maroulis computed $E=-1.15$ $Å^5$. This shows that for CF_4 the most recent values of A and E computed *ab initio* [6,7] are compatible with both isotropic (this work) and depolarized CIS data [5]. However, with these A and E values, the theoretical intensities referring to the highest frequencies lie below the experimental ones (beyond 50 and 120 cm^{-1} for depolarized and isotropic spectra, respectively). This behavior may be in part due to some short-range contributions that are not yet known in the case of CF_4 (such as exchange and overlap effects, molecular frame distortion, and/or spatial charge distribution of the non-point-like molecule) and are neglected in our model. The resulting doubt on the strong pure translational contribution to the *depolarized* spectrum cast a shadow on the accuracy of the ''depolarized spectrum fit'' of the $|A|$ and $|E|$ values made in previous works [26,5]. On the contrary, the weakness of the trace translational component implies that the $\alpha\mathsf{TA}$ (DIQ) and $\alpha\mathsf{TE}$ (DIO) mechanisms play the leading role in the isotropic spectrum and the isotropic spectrum fit of the $|A|$ and $|E|$ values can be considered as reliable below 120 cm^{-1} if we assume that (i) the rotational stick spectrum is mostly responsible for the spectral profiles of the latter mechanisms [15] and (ii) the absolute intensities of these dipole-multipole contributions are mainly classical in the case of CF_4 and are not significantly affected by the choice of the available potentials, as we have observed. In conclusion, the isotropic CIS spectrum is a good tool of investigation to measure the CF_4 dipole-multipole independent components. The agreement between the Maroulis *ab initio* computations and the theoretical analysis made here encourages further isotropic CIS studies on other optically isotropic molecules.

ACKNOWLEDGMENTS

We wish to thank George Maroulis for sending us his results prior to publication and for his helpful discussion. This work has been supported in part by the University of Angers, in part by Grant No. 2 P03B 152 10 of the Polish Commission for Scientific Studies, and in part by Grant No. 6454 of French-Polish Scientific and Technological Cooperation Joint Projects.

APPENDIX

We consider the interaction energy of two perturbed molecules in the form [32]

$$U=\sum_{l_1,l_2}\left(\frac{2^{l_1+l_2}}{(2l_1)!(2l_2)!}\right)^{1/2}\frac{X_N}{X_{l_2}} \times\{[\mathsf{Q}_{l_1}(1)\otimes\mathsf{T}_N(\mathsf{R}_{12})]_{l_2}\odot\mathsf{Q}_{l_2}(2)\}, \tag{A1}$$

where $N=l_1+l_2$, $X_{a,b\ldots f}=[(2a+1)(2b+1)\ldots(2f+1)]^{1/2}$, $\mathsf{Q}_{l_1}(i)$ denotes the l_ith-order spherical multipole moment of molecule i, and $\mathsf{T}_N(\mathsf{R}_{12})$ denotes the spherical interaction tensor

$$\mathsf{T}_N(\mathsf{R}_{12})=(-1)^N\left(\frac{(2N)!}{2^N}\right)^{1/2}\sqrt{\frac{4\pi}{2N+1}}\,R_{12}^{-(N+1)}\mathsf{Y}_N(\hat{\mathsf{R}}_{12}). \tag{A2}$$

The multipole moment of a perturbed molecule i can be written as the expansion [33]

$$Q_{k_1}^{n_1}(i)=Q_{k_1}^{n_1}(i,0)+\sum_{k_2,n_2}\overline{\alpha}_{k_1k_2}^{n_1n_2}(i,0)V_{k_2}^{n_2*}+\cdots, \tag{A3}$$

where $Q_{k_i}^{n_1}(i,0)$ and $\overline{\alpha}_{k_1k_2}^{n_1n_2}(i,0)$ denote, respectively, the multipole moment and symmetrized spherical reducible k_1th-k_2th-order multipole polarizability of an unperturbed molecule i and V_k stands for the kth-order regular solid spherical harmonic. The symbol 0 indicates here the multipole moment and the polarizability of an unperturbed (isolated) molecule. Further on, to simplify notation, we drop the 0.

Using Eqs. (A1) and (A3), we calculate the excess reducible dipolar pair polarizability tensor as the derivative

$$\Delta A_{11}^{m_1m_2}=-\left(\frac{\partial^2 U}{\partial V_1^{m_1*}\partial V_1^{m_2*}}\right)_{V\to 0} \tag{A4}$$

and, consequently, taking into account the multipolar contributions in Eq. (A3), we have

$$\begin{aligned}\Delta A_{11}^{m_1m_2}=&-\sum_{l_1,l_2}\left(\frac{2^{l_1+l_2}}{(2l_1)!(2l_2)!}\right)^{1/2}\frac{X_N}{X_{l_2}}\\&\times\sum_{\alpha,\beta,\gamma}\{(-1)^{\alpha}C_{l_1\beta N\gamma}^{l_2\alpha}\\&\times[\overline{\alpha}_{l_1 1}^{\beta m_1}(1)T_{N\gamma}(\mathsf{R}_{12})\overline{\alpha}_{l_2 1}^{\ \alpha m_2}(2)\\&+\overline{\alpha}_{l_1 1}^{\beta m_2}(1)T_{N\gamma}(\mathsf{R}_{12})\overline{\alpha}_{l_2 1}^{\ \alpha m_1}(2)]\},\end{aligned} \tag{A5}$$

where $C_{a\alpha b\beta}^{c\gamma}$ is the Clebsch-Gordan coefficient [13]. With the notation used elsewhere this Clebsch-Gordan coefficient compares as $C_{a\alpha b\beta}^{c\gamma}\equiv C(abc;\alpha\beta\gamma)$.

All polarizability tensors in Eqs. (A3)–(A5) are reducible under the three-dimensional rotation group. Irreducible tensors may be constructed from them by the standard coupling method

$$\overline{\alpha}_{l_1 1}^{\beta m_1}=\sum_{j_1,\phi}C_{l_1\beta 1m_1}^{j_1\phi}\alpha_{j_1\phi}^{(1l_1)}, \tag{A6}$$

$$\overline{\alpha}_{l_2 1}^{\ \alpha m_2}=\sum_{j_2,\eta}C_{l_2-\alpha 1m_2}^{j_2\eta}\alpha_{j_2\eta}^{(1l_2)}, \tag{A7}$$

$$\Delta A_{KM}^{(1,1)}=\sum_{m_1,m_2}C_{1m_1 1m_2}^{KM}\Delta A_{11}^{m_1m_2}. \tag{A8}$$

The sum of four Clebsch-Gordan coefficients of Eq. (A5) reduces to [13]

$$\begin{aligned}&\sum_{\substack{\alpha,\beta\\ m_1,m_2}}(-1)^{\alpha}C_{l_1\beta N\gamma}^{l_2\alpha}C_{l_1\beta 1m_1}^{j_1\phi}C_{l_2-\alpha 1m_2}^{j_2\eta}C_{1m_1 1m_2}^{KM}\\&\quad=(-1)^{j_1+j_2+L+N+l_2}X_{j_1j_2l_2}\\&\qquad\times\sum_{x,\xi}X_x C_{j_1\phi j_2\eta}^{x-\xi}C_{x-\xi N\gamma}^{KM}\begin{Bmatrix}j_1&j_2&x\\1&1&K\\l_1&l_2&N\end{Bmatrix}.\end{aligned} \tag{A9}$$

In the absence of magnetic effects the wave functions used in calculating the multipolar molecular polarizabilities can be chosen to be real [32]. This implies the symmetry relation $\alpha_{j_n}^{(k_1k_2)}=\alpha_{j_n}^{(k_2k_1)}$ and a sum $j_n+k_1+k_2$ to be even. Finally, for the excess interaction-induced irreducible spherical multipole pair polarizability tensor we have

$$\begin{aligned}\Delta A_{KM}=&2\sum_{\substack{j_1,j_2,x\\ l_1,l_2}}(-1)^{j_1+N}\left(\frac{2^N}{(2l_1)!(2l_2)!}\right)^{1/2}\\&\times X_{j_1j_2Nx}\begin{Bmatrix}j_1&j_2&x\\1&1&K\\l_1&l_2&N\end{Bmatrix}\{\mathsf{T}_N(\mathsf{R}_{12})\\&\otimes[\alpha_{j_1}^{(1l_1)}(1)\otimes\alpha_{j_2}^{(1l_2)}(2)]_x\}_{KM}.\end{aligned} \tag{A10}$$

Our derivation applies to static pair polarizability. We note, however, that the dynamic pair polarizability ΔA_{KM} formula derived by us previously [34] for nonabsorbing media has the same structure as Eq. (A10). Both pair polarizability formulas differ only by the fact that in the dynamic pair polarizability the dynamic *molecular* multipolar polarizabilities stand in place of the static ones of Eq. (A10).

By Eqs. (A10) and (A2) the excess interaction-induced pair polarizability in the space-fixed laboratory frame can be written in the form

$$\begin{aligned}\Delta A_{KM}=&\sqrt{4\pi}\sum_{\substack{j_1,j_2,N\\ l_1,l_2}}A_{j_1j_2xN}^{(K)}R_{12}^{-(N+1)}\\&\times\{\mathsf{Y}_N(\mathsf{R}_{12})\otimes[\alpha_{j_1}^{(1,l_1)}(1)\otimes\alpha_{j_2}^{(1,l_2)}(2)]_x\}_{KM}.\end{aligned} \tag{A11}$$

The transformation

$$\alpha_{j_1m_1}^{(1,l_1)}(i)=\sum_{m_1'}D_{m_1m_1'}^{j_1*}(\Omega_i)\tilde{\alpha}_{j_1m_1'}^{(1,l_1)}(i) \tag{A12}$$

defines the multipolar polarizability angular dependence in the laboratory frame. Within the R_{12}^{-7} range the following irreducible spherical components of molecular frame multipole polarizability are active in the description of ΔA_{KM}: (a) dipole-dipole, $\tilde{\alpha}_{00}^{(1,1)}=-\sqrt{3}\alpha$; (b) dipole-quadrupole, $\tilde{\alpha}_{3\pm 2}^{(1,2)}=\pm i\sqrt{2}A$; and (c) dipole-octopole, $\tilde{\alpha}_{40}^{(1,3)}=(\sqrt{7}/2)E$ and $\tilde{\alpha}_{4\pm 4}^{(1,3)}=(\sqrt{10}/4)E$. For the isotropic component of the excess pair polarizability ΔA_{00} the nonzero coefficients of Eq. (6) for the successive light scattering mechanisms have the following forms: $\alpha\mathsf{TA}$, $A_{3033}^{(0)}=-A_{0333}^{(0)}=-\frac{2}{3}\sqrt{15}$; $\alpha\mathsf{TE}$, $A_{4044}^{(0)}=A_{0444}^{(0)}=\frac{4}{3}\sqrt{7}$; ATA, $A_{3344}^{(0)}=-\frac{2}{3}\sqrt{154/3}$; ATE, $A_{4355}^{(0)}=-A_{3455}^{(0)}=2\sqrt{13}$; and ETE, $A_{4466}^{(0)}=\sqrt{165}$.

[1] *Collision- and Interaction-Induced Spectroscopy*, Vol. 452 of *NATO Advanced Study Institute, Series C: Mathematical and Physical Sciences*, edited by G. C. Tabisz and M. N. Neuman (Kluwer, Dordrecht, 1995).
[2] A. T. Prengel and W. S. Gornall, Phys. Rev. A **13**, 253 (1976).
[3] A. D. Buckingham and G. C. Tabisz, Mol. Phys. **36**, 583 (1978).
[4] F. Barocchi, A. Guasti, M. Zoppi, S. M. El-Sheikh, G. C. Tabisz, and N. Meinander, Phys. Rev. A **39**, 4537 (1989).
[5] A. Elliasmine, J.-L. Godet, Y. Le Duff, and T. Bancewicz, Mol. Phys. **90**, 147 (1997).
[6] G. Maroulis, Chem. Phys. Lett. **259**, 654 (1996).
[7] G. Maroulis, J. Chem. Phys. **105**, 8467 (1996).
[8] T. Bancewicz, V. Teboul, and Y. Le Duff, Phys. Rev. A **46**, 1349 (1992).
[9] J. H. Dymond and E. B. Smith, *The Virial Coefficient of Gases* (Clarendon, Oxford, 1969).
[10] B. J. Berne and R. Pecora, *Dynamic Light Scattering* (Wiley, New York, 1976).
[11] M. H. Proffitt, J. W. Keto, and L. Frommhold, Can. J. Phys. **59**, 1459 (1981).
[12] T. Bancewicz, V. Teboul, and Y. Le Duff, Mol. Phys. **81**, 1353 (1994).
[13] D. A. Varshalovich, A. N. Moskalev, and V. K. Khersonskii, *Kvantovaya Teoria Uglovogo Momenta* (Nauka, Moscow, 1975).
[14] H. Posch, Mol. Phys. **46**, 1213 (1982).
[15] N. Meinander, G. C. Tabisz, F. Barocchi, and M. Zoppi, Mol. Phys. **89**, 521 (1996).
[16] G. Birnbaum and E. R. Cohen, Can. J. Phys. **54**, 593 (1976).
[17] K. E. Cormack and W. G. Schneider, J. Chem. Phys. **19**, 849 (1951).
[18] A. E. Sherwood and J. M. Prausnitz, J. Chem. Phys. **41**, 429 (1964).
[19] G. C. Maitland, M. Rigby, E. B. Smith, and W. A. Wakeham, *Intermolecular Forces* (Clarendon, Oxford, 1981).
[20] C. G. Joslin, C. G. Gray, and Z. Gburski, Mol. Phys. **53**, 203 (1984).
[21] T. Bancewicz, Chem. Phys. Lett. **213**, 363 (1993).
[22] M. Moraldi, A. Borysow, and L. Frommhold, Chem. Phys. **86**, 339 (1984).
[23] Z. Lu and D. P. Shelton, J. Chem. Phys. **87**, 1967 (1987).
[24] T. Bancewicz, Chem. Phys. Lett. **244**, 305 (1995).
[25] H. E. Watson and K. L. Ramaswamy, Proc. R. Soc. London Ser. A **156**, 144 (1936).
[26] S. M. El-Sheikh and G. C. Tabisz, Mol. Phys. **68**, 1225 (1989).
[27] D. P. Shelton and G. C. Tabisz, Can. J. Phys. **59**, 1430 (1981).
[28] M. S. Brown, Shu-Kun Wang, and L. Frommhold, Phys. Rev. A **40**, 2276 (1989).
[29] F. Frommhold, Adv. Chem. Phys. **46**, 1 (1981).
[30] M. S. Brown and L. Frommhold, Mol. Phys. **66**, 527 (1989).
[31] F. Frommhold, J. D. Poll, and R. H. Tipping, Phys. Rev. A **46**, 2955 (1992).
[32] C. G. Gray and K. E. Gubbins, *Theory of Molecular Fluids. Vol. 1: Fundamentals* (Clarendon, Oxford, 1984).
[33] C. G. Gray and B. W. N. Lo, Chem. Phys. **14**, 73 (1976).
[34] T. Bancewicz, W. Głaz, and S. Kielich, Chem. Phys. **128**, 321 (1988).